Molecular-dynamics study of the binding energy and melting of transition-metal clusters

C. Rey, L. J. Gallego,* and J. García-Rodeja

Departamento de Física de la Materia Condensada, Facultad de Física, Universidad de Santiago de Compostela,
Santiago de Compostela, Spain

J. A. Alonso and M. P. Iñiguez

Departamento de Física Teórica, Facultad de Ciencias, Universidad de Valladolid, Valladolid, Spain

Using constant-energy molecular-dynamics simulations, we have studied the binding energies and melting behavior of Ni_N, Pd_N, Au_N, and Ag_N clusters ($N = 2$–23) on the basis of the embedded-atom model and the second-moment approximation to the tight-binding method. The results show that the applicability of these two models, which have proved to be very useful for interpreting surface and bulk properties of transition metals, is questionable for systems with few particles. It is also shown that the kind of empirical data used in computing the parameters of the model potentials can crucially influence the cluster results.

I. INTRODUCTION

The structural and dynamical properties of van der Waals clusters have been extensively studied in the last few years by molecular-dynamics (MD) and Monte Carlo simulations (see, e.g., Refs. 1–5). Work on ionic[6,7] and covalent[8,9] clusters has also been carried out. Results on metal clusters using these techniques are scarcer, although this is currently a subject of intense research.[10–18] This is due to the fact that many-body effects play an important role in metallic cohesion, i.e., complex interatomic potentials must be used. In fact, a fundamental question is whether the model potentials which are currently applied to bulk materials (see, e.g., Refs. 19 and 20) are accurate enough to describe the peculiar features of metallic systems with few particles.

Several papers on transition-metal clusters have recently been published. For instance, MD simulations have been used by Güvenç, Jellinek, and Voter[15] to study the melting behavior of Ni_N clusters ($N = 12$, 13, 14, and 19) on the basis of the Voter and Chen approach[21] to the embedded-atom model (EAM), by Garzón and Jellinek[13] to analyze the melting of Au_N clusters ($N = 6$, 7, and 13) using a Guptalike potential expressed in reduced units form, and by Valkealahti and Manninen[18] to study Cu clusters using the effective-medium (EM) theory.[22–25] Güvenç, Jellinek, and Voter[15] found a premelting phenomenon in Ni_{14} clusters, and that the relative difference between the melting points of Ni_{13} and bulk nickel was much smaller than for Lennard-Jones clusters.[1–5] However, there are no experimental results with which to compare these findings, and the studies of Au and Cu found larger reductions in melting points (which in the case of Au was similar to that observed experimentally, albeit for larger Au clusters[26,27]).

To gain more insight into transition-metal clusters and into the applicability of some of the available models of metal cohesion to this kind of system, in the present work we carried out an MD study of the binding energies, structures, and melting behavior of Ni, Pd, Ag, and Au

clusters in the size range $N = 2$–23. In the case of Ni, theoretical cluster structure results can be compared with empirical findings based on careful analysis of chemical reactivity for a wide range of sizes,[28] though it should be borne in mind that chemical reactions used to probe the structure of clusters may induce structural changes. Our results for Ni and Pd will also be compared with those obtained by Stave and DePristo[17] for $N = 4$–23 using a corrected effective-medium (CEM) model.

Several model potentials will be used in this paper. First, we shall consider the EAM, originally proposed by Daw and Baskes[29,30] on the basis of an earlier theory, the quasiatom[31] [or EM (Refs. 22 and 23)] approach. The EAM, which basically assumes that the total energy of the system is the sum of the energy necessary to embed each atom in the background electron density setup by the neighboring atoms (the "embedding energy") and an energy from two-body interactions, has been successfully applied to such problems as defects in metals,[30,32] surfaces,[30,33] alloys,[32] fracture[30,34] and the structure of liquid metals.[35] There are several semiempirical versions of the EAM which differ in the form of the functions involved and on the method used for their parametrization. Here, we shall mainly use the prescriptions of Foiles, Baskes, and Daw,[32] who proposed a set of embedding functions and pair interactions that allow a description of the pure fcc metals Ni, Pd, Pt, Cu, Ag, and Au and their alloys. For Ni clusters, however, we shall also use the Voter and Chen EAM approach,[21] which differs from the approach of Foiles, Baskes, and Daw primarily in that the core-core pair interaction has an attractive tail contribution (whereas in the version of Foiles, Baskes, and Daw it is entirely repulsive) and that properties of the diatomic molecule were used in fitting the embedding function and pair interaction. The EAM has been used with the parametrization suggested by Adams, Foiles, and Wolfer[36] to study the structures of large Ni clusters,[37] but its accuracy for small clusters is insufficiently tested.

As a second approach, we shall employ an N-body potential constructed using the second-moment approxima-

tion to the tight-binding method (TBM),[38] which has recently been employed by Massobrio, Pontikis, and Martin[39,40] in MD simulations of the crystal-to-amorphous transformation induced in the intermetallic compound $NiZr_2$ by the introduction of chemical disorder. This kind of potential has also been shown to reproduce the structural, bulk, and surface properties of fcc metals successfully.[41-43] The Guptalike potential used by Garzón and Jellinek[13] (see also Ref. 14) to study small transition-metal clusters is also based on the tight-binding method; however, since it is expressed in the form of reduced units, it does not by itself allow energetic and structural data to be obtained in absolute units.

Note that although the physical rationales of the EAM and TBM are quite different,[19,20] their governing equations are formally equivalent and have in common that the interaction between two atoms depends upon their local environment. They differ in that the TBM gives an explicit expression for the cohesive energy of the system (which facilitates its use in MD simulations), whereas the EAM embedding function must be constructed numerically once the pairwise potential and the electron density are known.

This paper is organized as follows. In Sec. II we briefly describe the ingredients of the model potentials used in our calculations. In Sec. III we give details of the MD simulations carried out, and present and discuss the calculated binding energies, structures, and melting behavior of the clusters studied. Finally, the main conclusions of this paper are summarized in Sec. IV.

II. MODEL POTENTIALS

In the EAM,[21,29,30,32-36] the total energy of a system of atoms is written as

$$E = \sum_i \left[F_i(\bar{\rho}_i) + \frac{1}{2} \sum_{j(\neq i)} \phi_{ij}(R_{ij}) \right] , \tag{1}$$

where $F_i(\bar{\rho}_i)$ is the energy required to embed atom i into the background electron density at site i, $\bar{\rho}_i$, and $\phi_{ij}(R_{ij})$ is the core-core pair interaction between atoms i and j separated by the distance R_{ij}. The host electron density $\bar{\rho}_i$ is approximated by linear superposition of the spherically averaged electron densities of all the atoms surrounding atom i,

$$\bar{\rho}_i = \sum_{j(\neq i)} \rho(R_{ij}) , \tag{2}$$

where $\rho(R_{ij})$ is the electron density of atom j at a distance R_{ij} from the nucleus. If the atomic densities $\rho(R)$ and the pair interaction $\phi(R)$ are both known, the embedding energy can be uniquely defined by requiring that the total energy given by Eq. (1) match the "universal" equation of state proposed by Rose et al.,[44] which gives the cohesive energy of the metal as a function of the lattice constant. The construction of $F(\bar{\rho})$ can then be performed numerically.

In the version of the EAM used by Foiles, Baskes, and Daw[32] (henceforth denoted EAM1), the atomic densities are obtained from the Hartree-Fock calculations of Clementi and Roetti[45] and MacLean and MacLean[46] by writing

$$\rho(R) = n_s \rho_s(R) + (n - n_s)\rho_d(R) , \tag{3}$$

where n is the total number of outer (s plus d) electrons, n_s is a measure of the number of outer s electrons, and ρ_s and ρ_d are the partial densities associated with the s and d wave functions, respectively. The atomic density of each metal is thus a function of the single parameter n_s, which allows for variations of the relative proportions of s and d electrons with respect to the electronic configuration of the free atom. The pair interaction is written as a short-range, purely repulsive potential of the form

$$\phi(R) = \frac{Z_0^2}{R}(1 + \beta R^\nu)^2 e^{-2\alpha R} , \tag{4}$$

where Z_0 corresponds to n, the number of outer electrons of the atom, and the parameters α, β, and ν were taken as adjustable. Foiles, Baskes, and Daw[32] determined α, β, ν, and n_s for the set of fcc metals Ni, Pd, Pt, Cu, Ag, and Au by optimizing for the prediction of the experimental data for the elastic constants and vacancy formation energies of the pure metals and for the heats of solution of the associated binary alloys, when information on the latter was available. This procedure ensures perfect agreement with equilibrium lattice constants, cohesive energies, and bulk moduli. The values of the parameters thus obtained for Ni, Pd, Ag, and Au (which we have chosen as an illustrative sample of the set of fcc transition metals considered by Foiles, Baskes, and Daw will be used in the cluster calculations of this paper. To be suitable for use in MD simulations, we have described the embedding functions corresponding to these four elements by cubic splines.

In the case of Ni, Voter and Chen[21] have used a rather different EAM procedure (henceforth referred to as EAM2). The electron density is parametrized as

$$\rho(R) = R^6(e^{-\beta R} + 2^9 e^{-2\beta R}) , \tag{5}$$

β being an adjustable parameter, and the core-core interaction is described by the Morse potential

$$\phi(R) = D_M\{1 - \exp[-\alpha_M(R - R_M)]\}^2 - D_M , \tag{6}$$

where D_M, R_M, and α_M are, respectively, the depth of the potential, the distance to the minimum, and a measure of the curvature at the minimum. D_M, R_M, α_M, β, and the cutoff distances R_{cut}, at which the functions $\phi(R)$ and $\rho(R)$ and their derivatives are forced to go smoothly to zero, were determined by Voter and Chen by minimizing the root-mean-square deviation between the calculated and experimental values of the elastic constants and vacancy formation energy of Ni metal and of the bond length and bond energy of the diatomic molecule. For comparison, the calculated values of these parameters (and the resulting embedding function, which we have represented by a cubic spline), have also been used in our MD study of Ni clusters.

As an alternative to the EAM, we have also investigat-

TABLE I. Experimental data (after Refs. 21 and 32) used to determine the TBM potential parameters and calculated (fitted) values. The equilibrium lattice constant of the metals a_0 and the bond length of the Ni dimer R_d are expressed in Å; the cohesive energy of the metals E_{coh} and the bond energy of the dimer E_d in eV; and the bulk modulus B and the elastic constants C_{11}, C_{12}, and C_{44} in units of 10^{12} ergs/cm^3.

	Ni			Pd		Au		Ag	
	Expt.	TBM1	TBM2	Expt.	TBM1	Expt.	TBM1	Expt.	TBM1
a_0	3.52			3.89		4.08		4.09	
E_{coh}	4.45	4.45	4.45	3.91	3.91	3.93	3.93	2.85	2.85
B	1.804	1.806	1.792	1.954	1.955	1.667	1.666	1.036	1.036
C_{11}	2.465	2.474	2.449	2.341	2.310	1.860	1.869	1.240	1.247
C_{12}	1.473	1.472	1.464	1.760	1.778	1.570	1.565	0.934	0.930
C_{44}	1.247	1.241	1.263	0.712	0.721	0.420	0.420	0.461	0.459
E_d	1.95	2.35	1.96						
R_d	2.20	2.33	2.40						

ed the behavior of Ni, Pd, Ag, and Au clusters assuming an N-body analytical potential constructed using the second-moment approximation to the TBM.[38] This potential, which was used by Massobrio, Pontikis, and Martin[39,40] to study the amorphization of the intermetallic al-NiZr$_2$ by MD simulation, is

$$E = \sum_i \left\{ \sum_{j(\neq i)} A \exp\left[-p\left(\frac{R_{ij}}{d} - 1\right)\right] - \left[\sum_{j(\neq i)} \xi^2 \exp\left[-2q\left(\frac{R_{ij}}{d} - 1\right)\right]\right]^{1/2} \right\},$$ (7)

where d is the nearest-neighbor distance in the bulk metal lattice and A, p, q, and ξ are adjustable parameters. The repulsive part of this potential is a Born-Mayer pairwise interaction and the attractive part arises from the TBM second-moment approximation to the electronic density of states. Using the software package MERLIN,[47] we have optimized these parameters for the prediction of the experimental values of the cohesive energy, bulk modulus, and elastic constants for each of the metals Ni, Pd, Ag, and Au while requiring the stable crystal structure to be fcc. For each metal, the cutoff radius R_c was optimized for overall agreement between the experimental and calculated data; all the resulting R_c's were large enough to avoid large discontinuities in the interatomic forces at the cutoff. We shall refer to this method of parametrization as TBM1. For Ni, we also carried out a second fit (TBM2) which includes the bond length and bond energy of the diatomic molecule among the optimization criteria. The experimental data used in the TBM fitting processes are listed in Table I along with the calculated data. The

values of the corresponding potential parameters for the metals Ni, Pd, Au, and Ag are shown in Table II.

III. COMPUTER SIMULATION, RESULTS AND DISCUSSION

The binding energies and melting behavior of Ni$_N$, Pd$_N$, Ag$_N$, and Au$_N$ clusters ($N = 2-23$) were investigated by microcanonical MD simulations using the velocity Verlet algorithm[48] with a time step of 10^{-15} s, which guarantees conservation of the total energy of the cluster to within 0.01%. The forces were computed analytically from the energies described by the EAM and the TBM [Eqs. (1) and (7)]. Initially, the clusters were prepared with zero total linear and angular momenta.

The structures with minimum energy were obtained using the steepest descent method.[49] In Figs. 1–4 we show, for Ni, Pd, Au, and Ag clusters, the binding energy [i.e., the total minimum energy $E(N)$ per atom with the opposite sign] and the second finite difference of the total energy

$$\Delta_2 E(N) = E(N+1) + E(N-1) - 2E(N) ,$$ (8)

calculated as a function of cluster size using the models described in Sec. II. A peak in $\Delta_2 E(N)$ indicates that the cluster of size N is more stable than neighboring clusters.

For Ni clusters, Fig. 1(a) shows that differences exist among the binding-energy results provided by the various models. EAM2 and TBM2, which have potential parameters calculated including diatomic data among the optimization criteria, predict lower binding energies than EAM1 and TBM1, respectively, which ignore diatomic data. However, all the models predict that Ni$_N$ clusters,

TABLE II. TBM potential parameters [see Eq. (7)] for the metals Ni, Pd, Au, and Ag (A and ξ in eV, R_c in Å).

	Ni (TBM1)	Ni (TBM2)	Pd (TBM1)	Au (TBM1)	Ag (TBM1)
A	0.046 5616	0.040 2543	0.173 750	0.222 356	0.106 026
p	15.0541	16.0902	10.8874	9.952 71	10.640 78
q	1.381 71	1.094 82	3.754 33	4.018 20	3.218 58
ξ	1.185 95	1.010 32	1.707 69	1.889 66	1.161 09
R_c	4.9780	6.5853	8.6983	9.1232	6.4669

such as Lennard-Jones clusters,[1-5] have peak stability for $N = 13$ and 19 [Fig. 1(b)]. Moreover, all the models predict that Ni clusters have structures based on icosahedral packing. In particular, Ni_{13} and Ni_{19} have icosahedral and double icosahedral configurations, respectively. The same basic geometrical configuration has been deduced by Stave and DePristo[17] for Ni clusters in the size range $N = 4-23$ using a CEM theory, and icosahedral growth has also been inferred for Ni clusters from 49 to at least 105 atoms on the basis of experimental adsorbate binding data[28] (this experimental method is unreliable for small clusters because the adsorbate can alter the cluster structure). EAM calculations with the parametrization of Adams, Foiles, and Wolfer[36] predict that icosahedral structures are energetically preferred for large Ni clusters containing less than $\simeq 2300$ atoms.[37] As well as our own results, Fig. 1(a) shows the CEM binding energies reported by Stave and DePristo and some *ab initio* results obtained for Ni_2, Ni_3, Ni_4, and Ni_6 clusters.[17] The EAM1 model, whose embedding function parameters were optimized[32] with respect to the bulk properties of pure Ni, Pd, Pt, Cu, Ag, and Au and the heats of solution of the associated binary alloys, affords binding energies much higher than the *ab initio* values. It appears, therefore,

that although the embedding functions of Foiles, Baskes, and Daw provide a good description of a wide range of bulk and surface properties of both the pure metals and their alloys,[32] they are not appropriate for the calculation of the binding energy of small clusters. In other words, the embedding function for embedding an atom in a small cluster is not the same as for embedding an atom in a bulk host of the same density. The EAM2 results seem to be more accurate because diatomic data were taken into account in optimizing the potential parameters. The CEM results, which virtually coincide with our TBM1 results, also appear to be much better than the EAM1 data, probably because the CEM accounts better for the effects of electron-density inhomogeneities in small systems.

For Pd, Au, and Ag we performed EAM1, TBM1, and TBM2 calculations, but since TBM failed to allow reasonable fit to both bulk and diatomic data, only the EAM1 and TBM1 results are discussed in what follows. For Pd (Fig. 2), EAM1 and TBM1 give very similar binding energies and reproduce the same icosahedral packing as found for Ni clusters, but only TBM1 gives a $\Delta_2 E$ peak for $N = 13$ (and perhaps for $N = 19$). Therefore, if marked stability for 13- and 19-atom clusters is expected to be a general characteristic of transition metals, EAM1
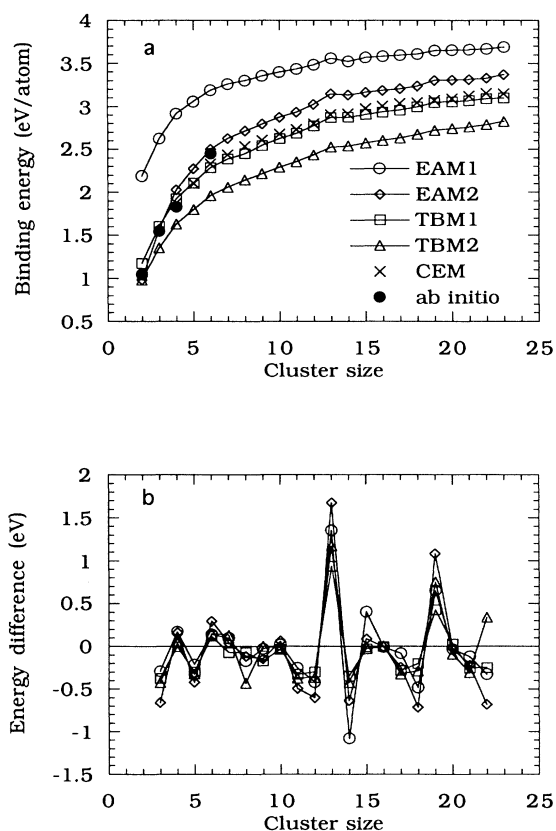
FIG. 1. Calculated Ni_N binding energies (a) and second finite differences of the total energies (b) as a function of cluster size. For comparison, the *ab initio* and CEM values reported by Stave and DePristo (Ref. 17) are shown in (a) (solid circles and crosses, respectively).
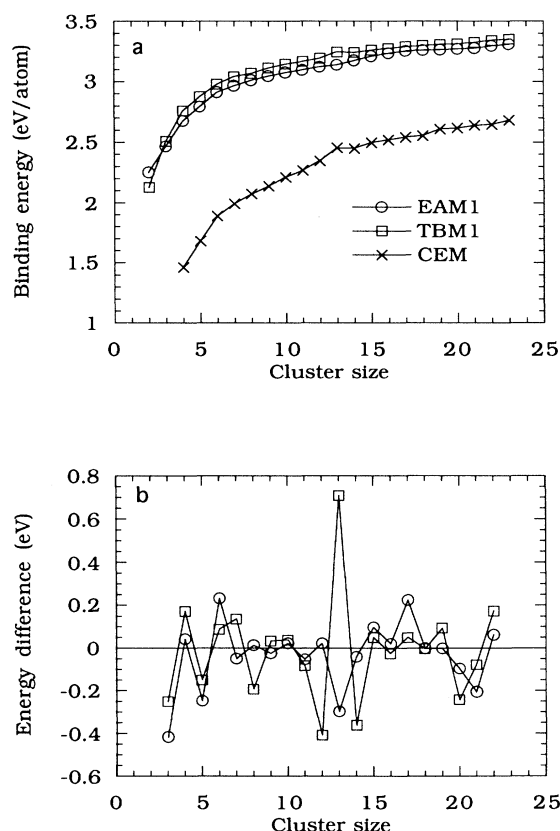
FIG. 2. Calculated Pd_N binding energies (a) and second finite differences of the total energies (b) as a function of cluster size. For comparison, the CEM values reported by Stave and DePristo (Ref. 17) are included in (a) (crosses).

must again be deemed to have been inadequate. Both the EAM1 and the TBM1 binding energies are considerably higher than the CEM values [Fig. 2(a)], which for the reasons indicated above are more accurate [as is corroborated by the experimental binding energy of Pd_2, 0.515 eV/atom (Ref. 50)].

The EAM1 and TBM1 results for Au are shown in Fig. 3. EAM1 fails to give $\Delta_2 E$ peaks and to reproduce icosahedral packing at $N = 13$ and 19, while TBM1 gives a peak at $N = 13$ associated with icosahedral structure, but not at $N = 19$ (for which a double icosahedral configuration is not reproduced). The binding energies predicted for the diatomic molecule Au_2 by EAM1 and TBM1 are both considerably larger than the experimental value, 1.145 eV/atom.[50]

For Ag clusters, EAM1 gave unreasonable predictions (e.g., that the atoms in the dimer are in close contact, with an extremely large binding energy). This reflects the inaccuracy of the EAM1 embedding energy, which is the term that provides the attractive contribution to the cohesive energy of the metal. TBM1, on the other hand, satisfactorily describes the enhanced, icosahedral stability of the Ag_{13} and Ag_{19} clusters [Fig. 4(b)], even though the calculated binding energies are probably somewhat large [1.361 eV/atom for Ag_2, as against the experimental value of 0.825 eV/atom (Ref. 50)].

The melting behavior of the clusters was investigated by gradually heating initial nonrotating, nontranslating structures to obtain the caloric curve (see Ref. 4 for details). Each state was allowed to propagate over 25×10^4 time steps, the first 5×10^4 for equilibration and the rest to obtain the corresponding caloric curve point by averaging the kinetic and potential energies (in the liquidlike region averages over 50×10^4 time steps were used because of the large thermodynamic fluctuations characteristic of systems with few particles). Next, all the velocities were scaled up by a factor of 1.1 and the resulting configuration used as input for the following iteration. The caloric curves obtained for 13- and 14-atom clusters are discussed below.

All the 13-atom clusters show melting behavior similar to that of Lennard-Jones clusters: when the energy is increased, the cluster changes from a rigid (solidlike) to a nonrigid (liquidlike) form via an intermediate stage. This is shown (Figs. 5–8) by the relative root-mean-square (rms) bond-length fluctuation δ, defined by[1]

$$\delta = \frac{2}{N(N-1)} \sum_{i<j} \frac{(\langle R_{ij}^2 \rangle - \langle R_{ij} \rangle^2)^{1/2}}{\langle R_{ij} \rangle} , \qquad (9)$$

where $\langle \ \rangle$ is the time average calculated over the entire

FIG. 3. Calculated Au_N binding energies (a) and second finite differences of the total energies (b) as a function of cluster size.
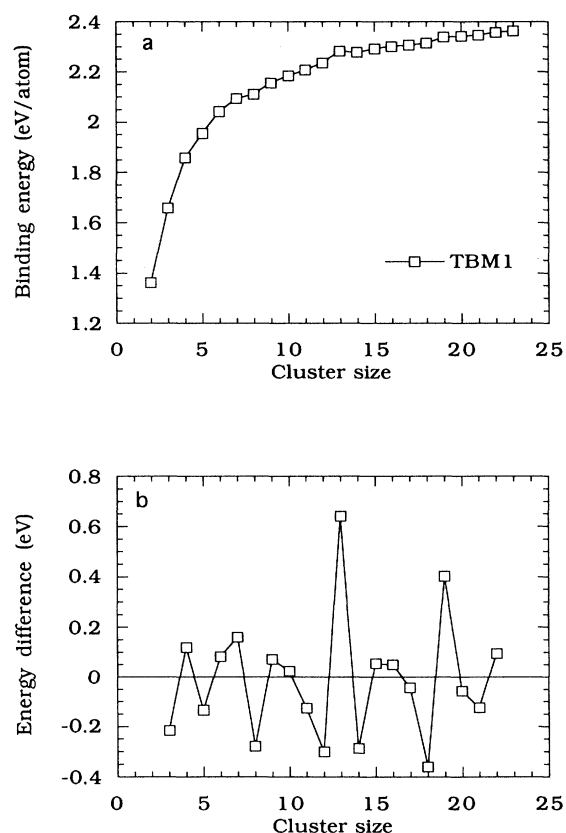
FIG. 4. Calculated Ag_N binding energies (a) and second finite differences of the total energies (b) as a function of cluster size.
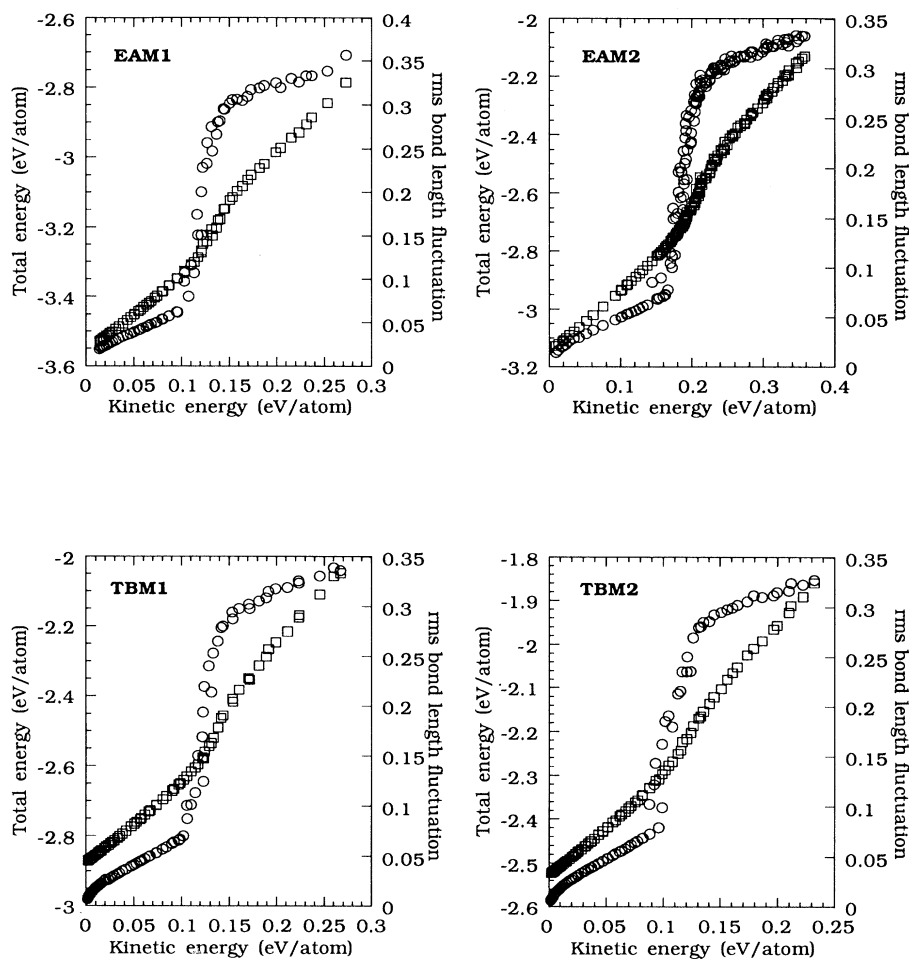
FIG. 5. Caloric curves for the Ni_{13} cluster. Squares represent total energy per atom (left scale), circles, rms bond-length fluctuations (right scale).

trajectory. For calculation of the melting temperature from[1]

$$T = \frac{2\langle E_{kin} \rangle}{k(3N-6)} \qquad (10)$$

(where k is the Boltzmann constant), the long-term average kinetic energy $\langle E_{kin} \rangle$ has in this work been taken to correspond to the middle of the transition region

($\delta \simeq 0.18$). The melting temperatures so calculated for the 13-atom clusters are listed in Table III together with those of the various bulk metals.[51] For Ni_{13}, EAM1, TBM1, and TBM2 predict rather similar large reductions of the melting temperature with respect to that of the bulk metal. EAM2, however, predicts a very small reduction, in agreement with previous EAM2-based MD simulations of Ni clusters by Güvenç, Jellinek, and
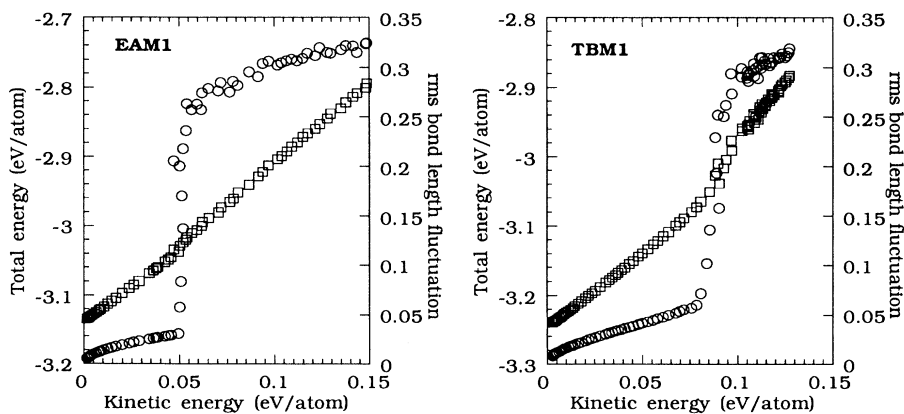
FIG. 6. Caloric curves for the Pd_{13} cluster. Squares represent total energy per atom (left scale), circles, rms bond-length fluctuations (right scale).
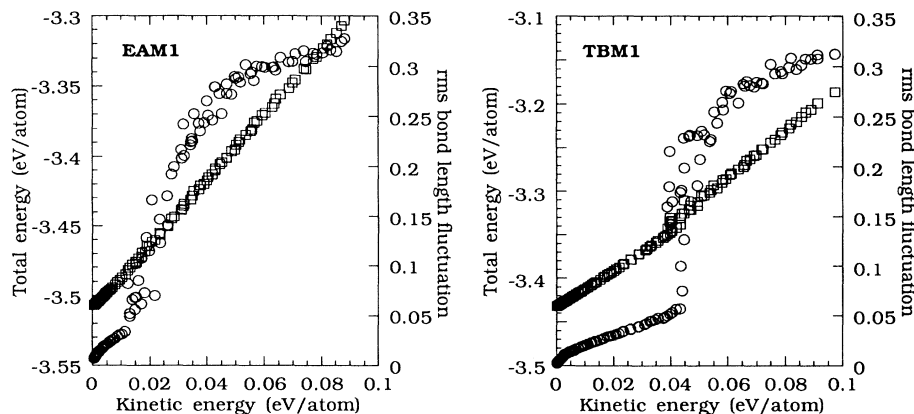
FIG. 7. Caloric curves for the Au_{13} cluster. Squares represent total energy per atom (left scale), circles, rms bond-length fluctuations (right scale).

Voter.[15]

In view of the results of EM-based calculations on the melting of Cu clusters, Valkealahti and Manninen[18] suggested the following equation for cluster melting temperature:

$$T_c = \frac{c_c}{c_b} T_b \;,$$ (11)

where T_c and T_b are the melting temperatures of the cluster and the bulk material, respectively, c_c is the mean coordination number of the atoms in the cluster, and c_b the corresponding bulk value ($c_b = 12$ for fcc metals). This equation implies that melting temperature falls rapidly with cluster size. The melting temperature predicted by Eq. (11) for Ni_{13} is in fairly good agreement with our EAM1, TBM1, and TBM2 results (Table III), and its prediction for Pd_{13} and Ag_{13} are similarly in keeping with the values given by TBM1 [which predicts the enhanced, icosahedral stability of Pd_{13} and Ag_{13} with respect to neighboring cluster sizes; see Figs. 2(b) and 4(b)] and, like these values, are well below the bulk melting temperatures. A still lower melting temperature is predicted for Pd_{13} by EAM1 (which fails to predict enhanced, icosahedral stability). For Au_{13}, very low melting tem-

peratures are predicted by both EAM1 and TBM1 (in spite of the latter's prediction of icosahedral stabilization).

The salient feature of the results for 14-atom clusters is the existence of a premelting state previously detected for Ni_{14} by Jellinek and Garzón[14] (using a Guptalike potential) and by Güvenç, Jellinek, and Voter[15] (for Ni_{14}, using EAM2). This phenomenon, which has no equivalent among Lennard-Jones clusters, implies a two-stage melting process. In general, this premelting phenomenon is shown by all our results for Ni_{14}, Pd_{14}, Au_{14}, and Ag_{14} (Figs. 9–12), the only exception being the EAM1 results for Au_{14}, which are similar to those for the 13-atom cluster (Fig. 7).

IV. SUMMARY AND CONCLUSIONS

In this work we calculated the binding energies and melting behavior of Ni, Pd, Au, and Ag clusters in the size range $N = 2$–23 using two of the current models of metallic cohesion, the embedded-atom model (EAM) and the tight-binding method (TBM), both of which have proved to be very useful for interpreting the surface and bulk properties of transition metals.[21,29,30,32–36,38–43] We used two different EAM parametrizations, EAM1 and EAM2: the former is due to Foiles, Baskes, and Daw,[32] who derived a set of "universal" embedding functions fitted to the bulk properties of the fcc metals Ni, Pd, Pt, Cu, Ag, and Au; the latter is the parametrization of Voter and Chen,[21] which differs from the parametrization
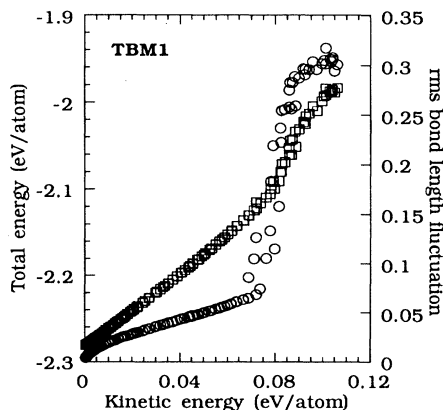
FIG. 8. Caloric curves for the Ag_{13} cluster. Squares represent total energy per atom (left scale), circles, rms bond-length fluctuations (right scale).

TABLE III. Calculated melting temperatures for the 13-atom clusters of the metals considered in this paper, together with the bulk melting temperatures (Ref. 51) T_b and the cluster melting temperatures T_{VM} obtained using Eq. (11) [proposed by Valkealahti and Manninen (Ref. 18)]. All data are in K.

	Ni	Pd	Au	Ag
EAM1	1118	468	247	
EAM2	1693			
TBM1	1117	816	413	732
TBM2	957			
T_b	1726	1825	1336	1234
T_{VM}	929	983	719	664
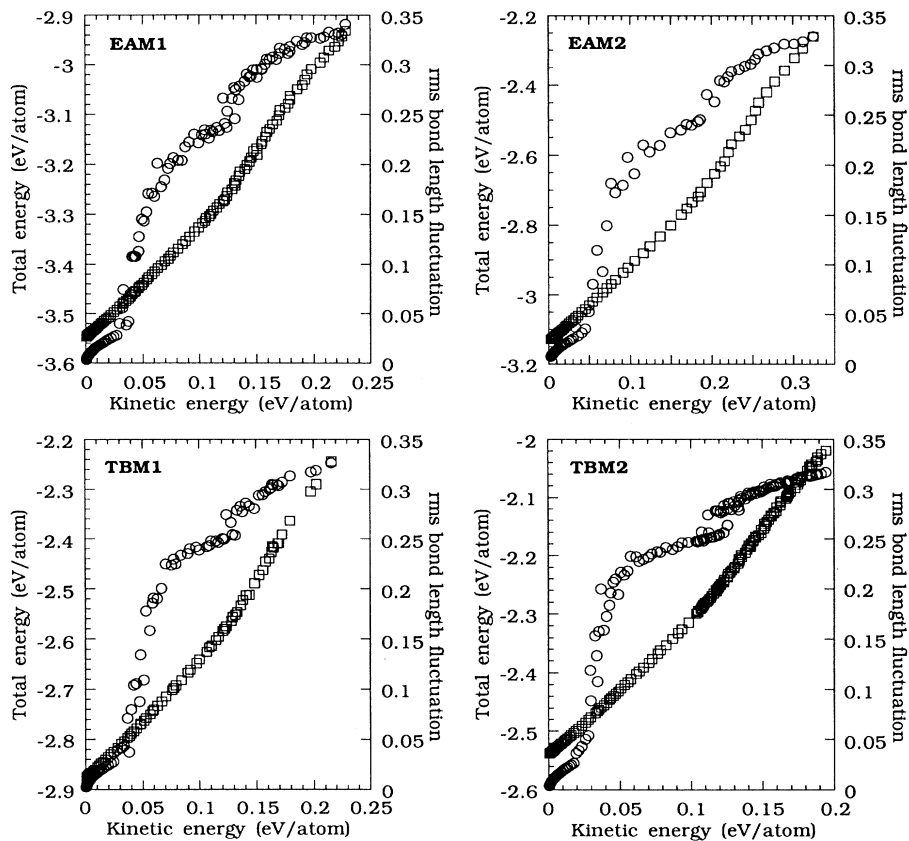
FIG. 9. Caloric curves for the Ni$_{14}$ cluster. Squares represent total energy per atom (left scale), circles, rms bond-length fluctuations (right scale).
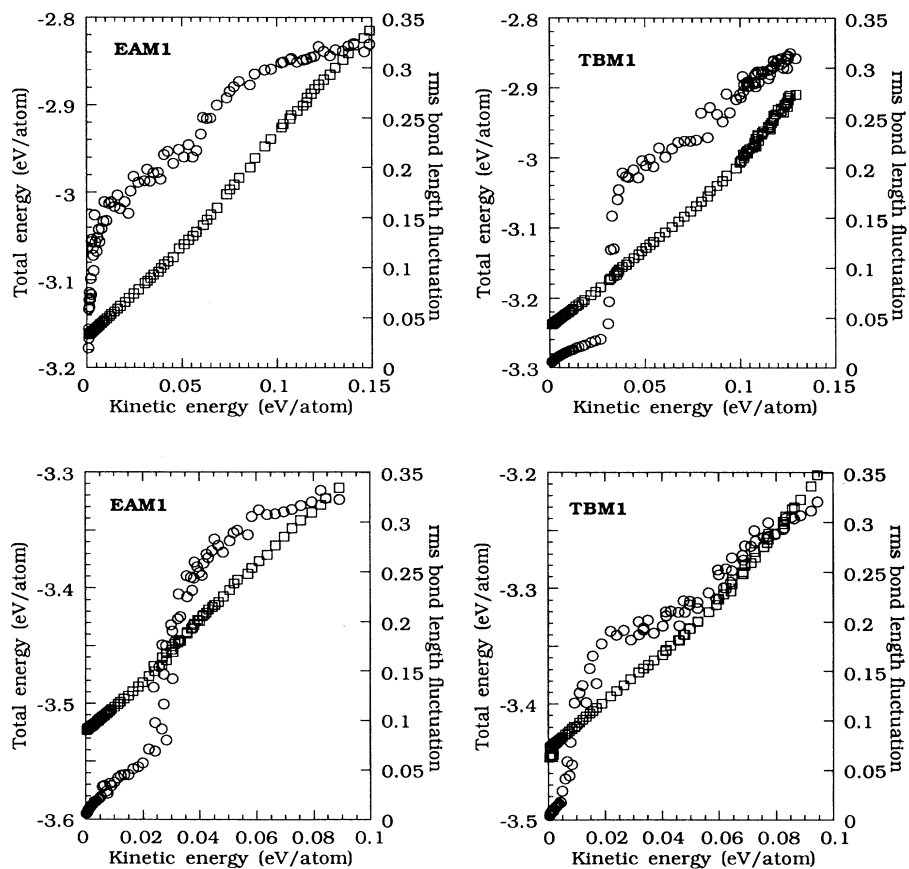
FIG. 10. Caloric curves for the Pd$_{14}$ cluster. Squares represent total energy per atom (left scale), circles, rms bond-length fluctuations (right scale).

FIG. 11. Caloric curves for the Au$_{14}$ cluster. Squares represent total energy per atom (left scale), circles, rms bond-length fluctuations (right scale).
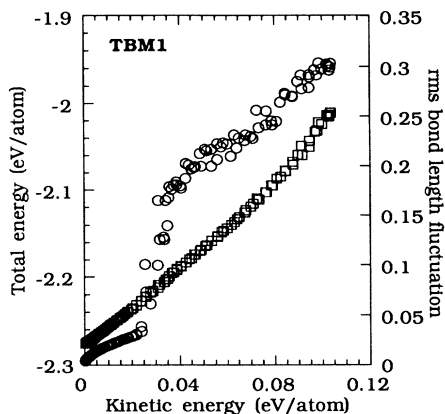
FIG. 12. Caloric curves for the Ag_{14} cluster. Squares represent total energy per atom (left scale), circles, rms bond-length fluctuations (right scale).

of Foiles, Baskes, and Daw primarily in the use a core-core pair interaction which has an attractive tail contribution (rather than being entirely repulsive) and the use of properties of the diatomic molecule in optimizing the embedding function and potential parameters. EAM2 was used only for Ni clusters. We also employed two different TBM approaches, TBM1 and TBM2, the former employing only basic bulk properties for fitting the potential and the latter including the bond length and bond energy of the diatomic molecule. The advantage of the TBM for MD simulations is that it provides a simple explicit expression for the cohesive energy of the system. The main aim of this work was to investigate the reliability of these theories for studying the behavior of small transition metal clusters. Our conclusions are as follows.

(a) EAM1 generally overestimates cluster binding energies, and only occasionally reproduces (e.g., for Ni) the expected enhanced stability of 13- and 19-atom clusters. These failings are mainly due to the use of a set of embedding functions fitted to the bulk properties of a set of pure fcc metals and their alloys,[32] i.e., to the assumption that the embedding function associated with each atom in a cluster is the same as the embedding function of an

atom in bulk metal of the same density. This assumption appears to be questionable, at least for the small transition-metal clusters studied here. In spite of this flaw, however, EAM1 successfully predicts the characteristic features of the melting behavior of Ni_{13} and Ni_{14}, yielding melting temperatures in good agreement with those obtained using the formula proposed by Valkealahti and Manninen.[18]

(b) EAM2, which includes diatomic data among the potential fitting criteria, yields more accurate cluster binding energies than EAM1, as shown by comparing with *ab initio* and CEM values for Ni clusters reported by Stave and DePristo.[17] In agreement with previous results of Güvenç, Jellinek, and Voter,[15] the calculated EAM2 melting temperature of Ni_{13} is very close to the bulk melting temperature.

(c) TBM1 generally overestimates cluster binding energies, although the values obtained for Ni clusters are very close to the available *ab initio* data and to the CEM values.[17] With the exception of Au clusters, TBM1 reproduces the enhanced stability of both 13- and 19-atom clusters, and predicts melting temperatures in fairly good agreement with those given by the equation of Valkealahti and Manninen.[18] For Pd, Au, and Ag clusters, this model cannot be fitted reasonably well to both bulk properties (cohesive energy and elastic constants) and diatomic properties (bond length and bond energy).

The above results thus show that the accuracy of two of the current models of metal cohesion, the EAM and the TBM, is questionable for systems with few particles, and that results can depend crucially on the kind of data to which the corresponding potentials are fitted. It is hoped that these findings may encourage further research leading to the refinement of metallic cohesion models for use in computer-simulation studies of the structural and dynamical properties of metal clusters.

ACKNOWLEDGMENTS

*Author to whom correspondence should be addressed.

[1] J. Jellinek, T. L. Beck, and R. S. Berry, J. Chem. Phys. **84**, 2783 (1986).

[2] H. L. Davis, J. Jellinek, and R. S. Berry, J. Chem. Phys. **86**, 6456 (1987).

[3] T. L. Beck, J. Jellinek, and R. S. Berry, J. Chem. Phys. **87**, 545 (1987).

[4] I. L. Garzón, M. Avalos-Borja, and E. Blaisten-Barojas, Phys. Rev. B **40**, 4749 (1989).

[5] D. J. Wales and R. S. Berry, J. Chem. Phys. **92**, 4283 (1990).

[6] J. Luo, U. Landman, and J. Jortner, in *Physics and Chemistry of Small Clusters*, Vol. 158 of *NATO Advanced Study Institute, Series B: Physics*, edited by P. Jena, B. K. Rao, and S. N. Khanna (Plenum, New York, 1987), p. 201.

[7] J. Jortner, D. Scharf, and U. Landman, in *Elemental and Molecular Clusters*, edited by G. Benedek, T. P. Martin, and G. Pacchioni (Springer-Verlag, Berlin, 1988), p. 148.

[8] E. Blaisten-Barojas and D. Levesque, Phys. Rev. B **34**, 3910 (1986).

[9] B. P. Feuston, R. K. Kalia, and P. Vashishta, Phys. Rev. B **35**, 6222 (1987).

[10] H. T. Diep, S. Sawada, and S. Sugano, Phys. Rev. B **39**, 9252 (1989).

[11] M. S. Stave, D. E. Sanders, T. J. Raeker, and A. E. DePristo, J. Chem. Phys. **93**, 4413 (1990).

[12] R. Kawai, and J. H. Weare, Phys. Rev. Lett. **65**, 80 (1990).

[13] I. L. Garzón and J. Jellinek, Z. Phys. D **20**, 235 (1991).

[14] J. Jellinek and I. L. Garzón, Z. Phys. D **20**, 239 (1991).

[15]Z. B. Güvenç, J. Jellinek, and A. F. Voter, in *Physics and Chemistry of Finite Systems: From Clusters to Crystals,* Vol. 374 of *NATO Advanced Study Institute, Series C: Mathematical and Physical Sciences,* edited by P. Jena, S. N. Khanna, and B. K. Rao (Kluwer, Dordrecht, 1992), p. 411.

[16]Z.-X. Cai, S. D. Mahanti, A. Antonelli, S. N. Khanna, and P. Jena, Phys. Rev. B **46**, 7841 (1992).

[17]M. S. Stave and A. E. DePristo, J. Chem. Phys. **97**, 3386 (1992).

[18]S. Valkealahti and M. Manninen, Phys. Rev. B **45**, 9459 (1992); (unpublished).

[19]*Atomistic Simulation of Materials Beyond Pair Potentials,* edited by V. Vitek and D. J. Srolovitz (Plenum, New York, 1989).

[20]*Many-Atom Interactions in Solids,* edited by R. M. Nieminen, M. J. Puska, and M. J. Manninen (Springer-Verlag, Berlin, 1990).

[21]A. F. Voter and S. P. Chen, in *Characterization of Defects in Materials,* edited by R. W. Siegal, J. R.Weertman, and R. Sinclair, MRS Symposia Proceedings No. 82 (Materials Research Society, Pittsburgh, 1987), p. 175.

[22]J. K. Nørskov and N. D. Lang, Phys. Rev. B **21**, 2131 (1980).

[23]J. K. Nørskov, Phys. Rev. B **26**, 2875 (1982).

[24]K. W. Jacobsen, J. K. Nørskov, and M. J. Puska, Phys. Rev. B **35**, 7423 (1987).

[25]H. Häkkinen and M. Manninen, J. Phys. Condens. Matter **1**, 9765 (1989).

[26]Ph. Buffat and J. P. Borel, Phys. Rev. A **13**, 2287 (1976).

[27]J. P. Borel, Surf. Sci. **106**, 1 (1981).

[28]E. K. Parks, B. J. Winter, T. D. Klots, and S. J. Riley, J. Chem. Phys. **94**, 1882 (1991).

[29]M. S. Daw and M. I. Baskes, Phys. Rev. Lett. **50**, 1285 (1983).

[30]M. S. Daw and M. I. Baskes, Phys. Rev. B **29**, 6443 (1984).

[31]M. J. Stott and E. Zaremba Phys. Rev. B **22**, 1564 (1980).

[32]S. M. Foiles, M. I. Baskes, and M. S. Daw, Phys. Rev. B **33**, 7983 (1986).

[33]M. S. Daw, Surf. Sci. Lett. **166**, L161 (1986).

[34]M. S. Daw, M. I. Baskes, C. L. Bisson, and W. G. Wolfer, in *Modelling Environmental Effects on Crack Growth Processes,* edited by R. H. Jones and W. W. Gerberich (The Metallurgical Society, Warrendale, PA, 1986).

[35]S. M. Foiles, Phys. Rev. B **32**, 3409 (1985).

[36]J. B. Adams, S. M. Foiles, and W. G. Wolfer, J. Mater. Res. **4**, 102 (1989).

[37]Ch. L. Cleveland and U. Landman, J. Chem. Phys. **94**, 7376 (1991).

[38]F. Ducastelle, J. Phys. (Paris) **31**, 1055 (1970).

[39]C. Massobrio, V. Pontikis, and G. Martin, Phys. Rev. Lett. **62**, 1142 (1989).

[40]C. Massobrio, V. Pontikis, and G. Martin, Phys. Rev. B **41**, 10 486 (1990).

[41]V. Rosato, M. Guillopé, and B. Legrand, Philos. Mag. A **59**, 321 (1989).

[42]M. Guillopé and B. Legrand, Surf. Sci. **215**, 577 (1989).

[43]B. Loisel, D. Gorse, V. Pontikis, and J. Lapujoulade, Surf. Sci. **221**, 365 (1989).

[44]J. H. Rose, J. R. Smith, F. Guinea, and J. Ferrante, Phys. Rev. B **29**, 2963 (1984).

[45]E. Clementi and C. Roetti, At. Data Nucl. Data Tables **14**, 177 (1974).

[46]A. D. MacLean and R. S. MacLean, At. Data Nucl. Data Tables **26**, 197 (1981).

[47]G. A. Evangelakis, J. P. Rizos, I. E. Lagaris, and I. N. Demetropoulos, Comput. Phys. Commun. **46**, 401 (1987).

[48]W. C. Swope, H. C. Andersen, P. H. Berens, and K. R. Wilson, J. Chem. Phys. **76**, 637 (1982).

[49]F. H. Stillinger and T. A. Weber, Phys. Rev. A **25**, 978 (1982).

[50]M. D. Morse, Chem. Rev. **86**, 1049 (1986).

[51]R. Hultgren, P. D. Desai, D. T. Hawkins, M. Gleiser, K. K. Kelley, and D. D. Wagman, *Selected Values of the Thermodynamic Properties of the Elements* (American Society for Metals, Metals, Park, OH, 1973).